-RESEARCH PAPER-

International Journal of Mining and Geo-Engineering

IJMGE

IJMGE 59-1 (2025) 75-81

DOI: 10.22059/IJMGE.2025.383755.595202

Investigating the alteration of igneous rocks in relation to bentonite mineral mapping using remote sensing data in Khor and Biabanak, central Iran

Jafar Norouzi [a, *], Hooshang Asadi Haroni [b], and Morteza Tabaei [b]

[a] *Department of Petroleum Engineering, Amirkabir University of Technology, Tehran, Iran.*

[b] *Department of Mining Engineering, Isfahan University of Technology, Isfahan, Iran.*

Article History:

Received: 20 October 2024.

Revised: 21 December 2024.

Accepted: 12 February 2025.

ABSTRACT

The alteration of igneous rocks indicates the formation and identification of valuable mineral deposits, such as bentonite, which is in increasing demand across various industries, including oil and steel. Remote sensing methods, leveraging the spectral characteristics of minerals, can detect hydrothermal alteration zones associated with various ore deposits, including bentonite, thereby reducing the cost of time and fieldwork. This study investigates the alteration of igneous rocks in the Khor and Biabanak region, located in the eastern part of Isfahan province, Iran, northeast of Nain city. Using ETM+ satellite data and field observations, we aimed to identify new potential bentonite resources. The ETM+ satellite data was processed using preprocessing stages including Layer Stacking, Subseting, Radiometric Corrections, Geometric Corrections, SLC-off Gap Filling, Noise Reduction (Destriping), Cloud and Water Masking, and Band Scaling/Normalization). This was followed by applying False Color Composite (FCC), Principal Component Analysis (PCA), the Enhanced Crosta technique, and the Least Squares Fitting (LS-Fit) method, which enabled us to identify promising mineral zones. Field surveys and X-ray Diffraction (XRD) analysis of samples confirmed significant concentrations of smectite (montmorillonite), indicative of substantial bentonite deposits. These findings suggest that integrating remote sensing techniques with field validation successfully identified areas with significant bentonite potential for further exploration. The successful application of these methods, particularly in a region with limited prior bentonite-focused remote sensing studies, highlights their utility in similar geological settings, offering a valuable approach for mineral exploration.

Keywords: *Crosta method, Igneous rocks alteration, Least squares fitting method, Mineral exploration, Remote sensing.*

1. Introduction

Remote sensing is a technique that measures objects from a distance without direct contact [1]. Remote sensing data can provide reflectance spectroscopic information that aids in locating mineral deposits and reducing the expenses and time of fieldwork studies [2, 3]. Remote sensing methods, especially those utilizing the spectral properties of minerals, have been effective in identifying hydrothermal alteration zones associated with various ore deposits, including bentonite [4, 5]. These techniques, especially when using ASTER data, have proven effective in mapping hydrothermal alteration zones, as demonstrated by studies [6, 7] in which good geological exposure allows for the direct identification of spectral signatures from rocks and soils. A key principle of mineral exploration is the increased likelihood of finding new deposits near existing ones. For example, if mining is occurring in a certain area, similar minerals are more likely to be found nearby, with the likelihood decreasing with distance. In this context, remote sensing can effectively identify areas with high potential for mineralization, primarily through multi- or hyperspectral remote sensing images [8, 9]. It is important to note that iron oxide minerals often co-occur with clay minerals, such as those found in bentonite within hydrothermal alteration zones. The processes that lead to the formation of bentonite can also result in the formation of iron oxides. Therefore, detecting areas with enhanced iron oxide signatures can be a valuable indicator when locating potential bentonite deposits.

Landsat 7, launched in April 1999, features the Enhanced Thematic Mapper Plus (ETM+). Its primary mission was to extend the data collection initiated by Landsat-4 and Landsat-5 TM. The sensor's bands 1 through 7, which encompass the blue, green, red, near infrared, and shortwave infrared spectra, correspond to those of the Landsat TM and have a ground resolution of 30 meters. This study utilized bands 1, 2, 3, 4, 5, and 7. The thermal infrared band of ETM+ (Band 6) had a ground resolution of 60 meters. Most types of studies can be sufficiently conducted with a spatial resolution of 30 meters [10]. However, this study did not use Band 6. Image processing techniques, such as band combination and ratioing, PCA, SAM, SID, MTMF, LSU, and CEM, were applied using the spectral data obtained from the satellites [11, 12].

Multispectral data frequently include bands with overlapping information. Principal Component Analysis (PCA) addresses this by analyzing the statistical properties of multi-band images; thus, eliminating redundant and unnecessary data [13]. PCA mitigates the impact of irradiance that affects all bands and enhances the reflectance characteristics of geological materials. This technique is applicable to multivariate datasets, such as multispectral images in remote sensing, to extract spectral signatures of specific minerals, including those related to hydrothermal alteration. The Crosta technique, a feature-oriented

* Corresponding author. *E-mail address:* j_norouzi@aut.ac.ir (J. Norouzi).

PCA method, relies on the correlation between the eigenvector matrix values used in PCA and the spectral responses of target materials. This approach identifies the principal components that encapsulate the spectral information of the target mineral, with the resulting pixel values represented as either dark or bright [14]. Many studies have successfully determined mineralization zones using PCA, proving its effectiveness compared to classical methods [12, 15-17].

The Crosta technique can be used with a selection of four to six multispectral bands from Landsat and ASTER satellite data. The choice of specific bands is based on their reflectance values. After conducting PCA, the most appropriate component was identified by analyzing how the newly created bands correlate with bands of high and low reflectivity. The reflectivity signs of these bands were then assessed. If the band with the highest reflectivity is positive, the eigenvector loading is positive, resulting in the target minerals appearing brighter. Conversely, if the highest-reflectivity band is negative, the eigenvector loading is negative. To improve the visibility of the minerals, the component was multiplied by -1. Crosta et al. (2003) utilized this approach to adapt PCA for detecting alunite, illite, kaolinite-smectite, and kaolinite in Patagonia, Argentina [14]. They employed the following band combinations: 1, 3, 5, 7 (with bands 1 and 5 showing low reflectance and bands 3 and 7 showing high reflectance) for alunite; 1, 3, 5, 6 (with bands 1 and 5 showing high reflectance and bands 3 and 6 showing low reflectance) for illite; 1, 4, 6, 9 (with bands 1 and 6 showing low reflectance and bands 4 and 9 showing high reflectance) for kaolinite-smectite; and 1, 4, 6, 7 (with bands 1 and 6 showing low reflectance and bands 4 and 7 showing high reflectance) for kaolinite.

2. Geographic location of the area

The study area covers approximately 400 square kilometers in the eastern part of Isfahan province, northeast of Nain city, within the Khor and Biabanak district. It is situated south of Khor city and north of Mehriz city, between latitudes 33°33'45" to 33°41'06" N and longitudes 55°15'07" to 55°25'09" E. This area can be observed on a 1:100,000 geological map (Fig. 1).

3. Geological characteristics of the area

The research site is situated in the Central Iran Zone. The oldest geological formations present in this area are part of the Upper Jurassic-Lower Cretaceous Chah Palang formation. These rocks, exposed in Kuh-e Matang, are characterized by variegated mud shale with sandstone interlayers [2].

These rocks are conformably overlain by the Neocomian Noqreh formation, which includes a variety of rock types, such as alternating quartz conglomerate, red and green sandstone, marl, limestone, and argillite, as well as individual lenses of gypsiferous clay or gypsum. The Noqreh formation is conformably overlain by the Shah Kuh formation [3].

The Shah Kuh formation primarily comprises orbitolina limestone but also includes marl and sandstone. This formation is exposed in Kuh-e Matang and in fault blocks to the southwest and east of it. Overlying the Shah Kuh formation's limestone is a sequence of weakly metamorphosed rocks comprising the Biabanak and Mirza formations. These formations are of particular interest due to their potential for hosting bentonite deposits.

The Biabanak formation is divided into two members: the lower one and the upper one. To the east of Kuh-e Howz-e Mirza, a member of flyschoid interstratified rocks is identified in the upper part of the formation. The Farrokhi formation is conformably overlain by the Paleocene Chupanan formation.

The Lower Eocene Darreh Anjir formation occurs with a sharp angular unconformity over the Lower Cretaceous rocks. This formation consists of intercalating conglomerate and sandstone, mudstone and marl, and limestone. In the eastern part of the area occupied by the Darreh Anjir formation, a 320 m red member is identified.

The Lower Eocene rocks rest on the rocks of the Darreh Anjir formation without apparent unconformity, but they show a sharp angular unconformity with older formations. These rocks are represented at the base mostly by tuffaceous conglomerate and upward by thinly intercalating tuff, tuffaceous sandstone, and tuffaceous siltstone. In the lower portions of the sequence, an essentially tuffaceous unit is singled out. The apparent thickness of the Lower Eocene volcanic rocks is about 200 meters. In the southeastern spurs of Kuh-e Matang pyroclastic rocks locally underwent hydrothermal alterations and were transformed into bentonite (up to 40 m thick) (Fig. 1) [2].

The presence of altered pyroclastic rocks transformed into bentonite in the southeastern spurs of Kuh-e Matang highlights the direct relevance of the region's geology to the study's objective.

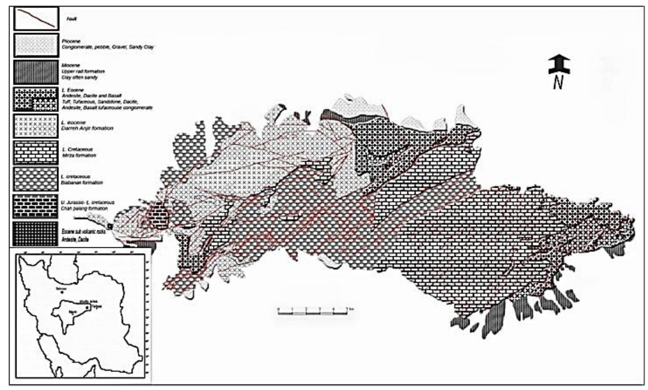

Fig. 1. The geological map of the area [2].

4. Satellite data of the study area

Landsat data have been a valuable tool in various earth sciences applications, since its inception and remains relevant today. In geological applications, it aids in locating minerals containing iron oxide and hydroxyl groups found in hydrothermally altered zones of mineral deposits, particularly in arid and semiarid regions. This makes it widely utilized in mine exploration studies, especially for identifying hydrothermal alteration zones.

The study area's hydrothermal alteration and iron oxide-enriched locations were analyzed using the principal component analysis (PCA), also known as the Crosta technique in remote sensing studies.

Wall rocks containing mineral deposits exhibit end products resulting from hydrothermal fluid reactions, which alter the rock's chemistry and lead to ore and hydrothermal mineral deposition. All porphyry-type deposits show well-developed zones that are distinguishable by differences in major oxides and trace element concentrations, which manifest as changes in the mineralogical composition of altered zones.

Hydrothermal alteration, a key process in the formation of many ore deposits, including bentonite, changes the mineralogical composition of the host rocks. These alterations often result in the formation of clay minerals (such as smectite, the primary component of bentonite) and iron oxides. Remote sensing techniques, particularly the PCA, are effective in mapping these alteration minerals by identifying diagnostic spectral features.

Landsat 7 ETM+ bands 1, 3, 5, and 7 are deemed appropriate for geological and exploration geology research. The analysis included general statistics, a correlation matrix, and PCA covariance eigenvector values for these Landsat 7 ETM+ bands. Specifically, bands 1, 3, 4, and 5 are sensitive to iron oxide minerals, while bands 1, 4, 5, and 7 are useful for detecting hydroxyl-bearing minerals, including clay minerals.

The study area is located in the UTM system in zone 40 South. Satellite data for this area have been acquired through the ETM sensor of the Landsat 7 satellite in seven bands. This dataset consists of three visible bands (blue, green, and red) along with one near-infrared band and two mid-infrared bands, all with a spatial resolution of 30 meters and reflective properties. Moreover, the dataset includes a thermal infrared band with a spatial resolution of 120 meters and emissive properties. While newer sensors, such as Landsat 8/9 OLI offer improved capabilities, ETM+ data was chosen for this study because of its availability and historical coverage for the Khor and Biabanak region. The selection of ETM+ data was driven by its archival availability and extensive temporal coverage for the Khor and Biabanak region, enabling potential future time-series analysis. Furthermore, the spectral range of ETM+ bands is suitable for detecting the key alteration minerals associated with bentonite deposits, namely hydroxyl-bearing minerals and iron oxides.

4.1. Data preprocessing

The Landsat 7 ETM+ data underwent several preprocessing steps to ensure accuracy and consistency in the analysis. These steps included Layer Stacking, Subsetting, Radiometric Corrections, Geometric Corrections, SLC-off Gap Filling, Noise Reduction (Destriping), Cloud and Water Masking, and Band Scaling/Normalization. During geometric correction, the ground control points (GCPs) and digital elevation model (DEM) were used to ensure sub-pixel accuracy. Radiometric correction involved converting the digital numbers to surface reflectance using appropriate atmospheric correction models. The SLC-off gaps were filled using a nearest neighbor interpolation technique.

After these preprocessing steps, the main image processing techniques for mineral mapping, such as PCA and LS-Fit, were performed. Table 1 presents the general statistics and correlation matrix values for the bands (1, 2, 3, 4, 5, and 7) utilized in the study.

Table 1. Correlation Matrix values of Landsat 7 ETM+ satellite image data for six bands.

Correlation Matrix	Band 1	Band 2	Band 3	Band 4	Band 5	Band 7
Band 1	1.000000	0.318319	0.931974	0.206149	0.140918	0.710243
Band 2	0.318319	1.000000	0.401794	0.979046	0.962496	0.319261
Band 3	0.931974	0.401794	1.000000	0.314253	0.249639	0.758419
Band 4	0.206149	0.979046	0.314253	1.000000	0.994295	0.283505
Band 5	0.140918	0.962496	0.249639	0.994295	1.000000	0.251874
Band 7	0.710243	0.319261	0.758419	0.283505	0.251874	1.000000

5. Remote sensing studies by geographic information systems

As previously noted, the role of remote sensing studies has grown significantly in supporting geological exploration for ore deposits. These studies enhance efficiency and streamline workflows by enabling disciplined data utilization with the aid of GIS, which allows for comprehensive multidimensional evaluations. In this study, GIS software (ENVI 5.3) was used for data processing, analysis, and visualization, facilitating the integration of remote sensing data with other spatial information.

The primary objective of this research was to delineate hydrothermally altered zones potentially associated with bentonite mineralization within the study area. To achieve this, we employed a combination of visual interpretation using False Color Composites (FCC) and spectral analysis techniques including Principal Component Analysis (PCA) and Least Squares Fitting (LS-Fit). While this study utilizes PCA and LS-Fit, other methods, such as the U-Statistic method and singularity methods in combination with fuzzy gamma operators, have also been successfully applied to delineate mineral potential zones from satellite imagery systems [18-20].

5.1. False color composite (FCC)

False color composites, such as the one used here, are valuable for visual interpretation of alteration zones and have been combined with techniques, such as singularity analysis for enhanced alteration mapping in other studies [21]. Referring to Figs. 2 and 3, previous research has shown that clay minerals exhibit the greatest reflectance in band 5 and the highest absorption in band 7, while iron oxides show peak reflectance in bands 3 and 5 and peak absorption in bands 1 and 4 [22]. Since plants have the highest reflectance in band 4 of ETM+ satellite data, vegetation will appear very clear and bright green in an RGB (741) color composite. As shown in Fig. 4, no significant vegetation cover is observed in the study area.

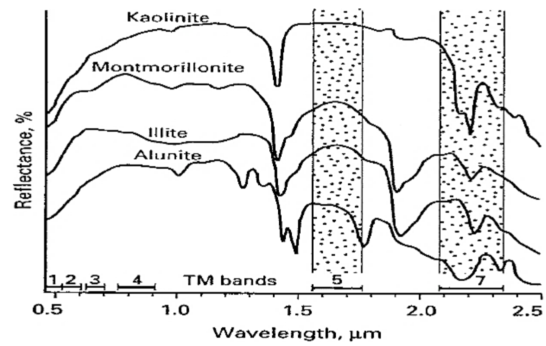

Fig. 2. Spectral reflectance for several typical clay minerals [1]

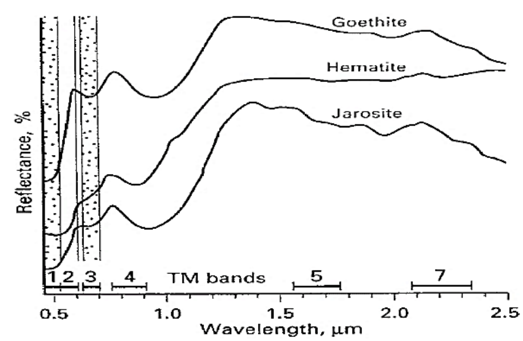

Fig. 3. Spectral reflectance for jarosite, hematite, and goethite [1].

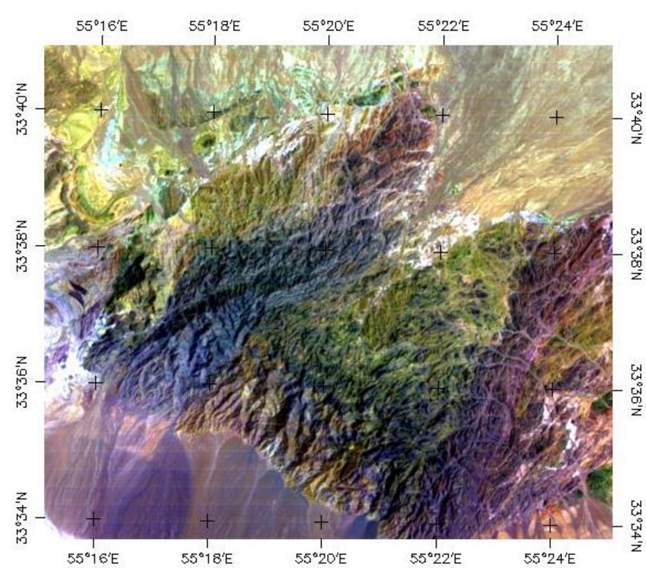

Fig. 4. RGB (741) color composite image of the study region.

5.2. Principal component analysis method (the Crosta method)

To gather spectral data linked to hydrothermal changes across a vast region, a reliable and tested image-processing method was selected: the Crosta method based on the PCA. This method was preferred for its ability to efficiently extract "clay + iron" spectral signatures using the limited spectral resolution of ETM+, relying solely on scene statistics without any prior geological knowledge of the area.

PCA was applied to a subset of bands 1, 3, 4, and 5 for both ETM+ scenes to collect spectral data associated with iron minerals (hematite, goethite, and jarosite), which are produced through the weathering of sulfides in epithermal environments. Additionally, the PCA was applied to the subset of bands 1, 4, 5, and 7 to extract spectral data related to hydroxyl-bearing minerals, such as kaolinite, illite, alunite, and other minerals typical of hydrothermally altered areas [15, 16]. In addition to PCA, fractal models, such as the CN fractal model can also be applied to ASTER images to delineate alteration zones [23].

5.2.1. Clay minerals alterations (OH type)

Bands, 7, 5, 4, and 1 were selected, since clay minerals in the spectral range of band 5 had reflective features and in the spectral range of band 7, they exhibited absorptive features and, band 3 was excluded to disregard iron oxides, and band 2 was eliminated due to its similarity to band 1.

The covariance matrix and principal component analysis for this band combination are presented in Table 2 and 3. According to Table 3, the highest difference between the eigenvalues of bands 5 and 7 was observed in PC4 (band 7: 0.415046 and band 5: -0.806558). Therefore, PC4 was chosen for clay minerals. This image, after negation and interactive stretching, is shown in Fig. 5. Bright points in the Fig. 5 not only indicate alterations in clay-rich areas but also highlight regions containing gypsum.

Table 2. The Covariance matrix values corresponding to bands 1, 4, 5, and 7.

Covariance Matrix	Band 1	Band 4	Band 5	Band 7
Band 1	650.588878	415.182147	429.920810	177.582231
Band 4	415.182147	2614.834448	371.583477	160.032234
Band 5	429.920810	371.583477	327.086325	134.455771
Band 7	177.582231	160.032234	134.455771	96.089957

Table 3. The PCA eigenvector matrix values for bands 1, 4, 5, and 7.

Eigenvector	Band 1	Band 4	Band 5	Band 7
PC 1	0.227905	0.952149	0.187019	0.080599
PC 2	-0.776017	0.303947	-0.507934	-0.217753
PC 3	-0.411301	-0.0227	0.23768	0.879673
PC 4	0.0420342	0.022676	-0.806558	0.415046

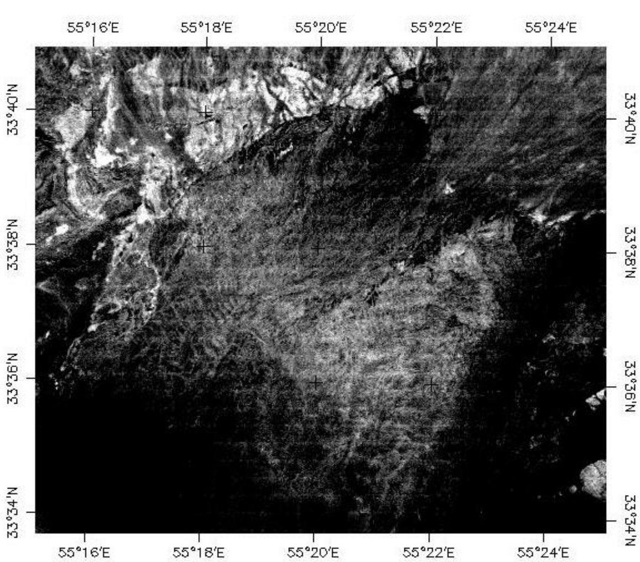

Fig. 5. PC4 image showcasing clay minerals, where altered regions are depicted as bright pixels.

5.2.2. Iron oxide mineral alterations

As discussed before, the bands 1-3-4-5 were selected for iron oxide mineral analysis. This was because iron oxides had strong reflectance properties in the spectral range of band 3 and strong absorption properties in the spectral range of band 1. The findings from the principal component analysis along with the matrix of eigenvectors of this band combination are shown in Table 4.

Table 4. The PCA eigenvector matrix values for bands 1, 3, 4, and 5.

Eigenvector	Band 1	Band 3	Band 4	Band 5
PC1	0.822915	0.119905	0.552773	0.053626
PC2	0.027727	-0.89255	0.191831	-0.40717
PC3	-0.33566	-0.25736	0.481031	0.767922
PC4	-0.45757	0.350349	0.65288	-0.49156

Table 4 reveals that the highest difference between bands 1 and 3 eigenvector values is observed in component PC2 (band 1 = +0.027727 and band 3 = -0.892549). Due to the sign of PC3, there is no need for inversion. The image of this PC after stretching in grayscale is shown in Fig. 6.

To identify points contaminated with clay minerals, the optimized Crosta technique was employed, and an RGB color combination was formed as follows: R=PC4(OH), G=PC3(OH), and B=PC2(Fe). In Fig. 7, points contaminated with OH-type alterations are displayed in red to orange color after interactive stretching.

5.3. LS-Fit method

5.3.1. Clay minerals alterations

To pinpoint areas of clay mineral alteration (OH type), the LS-Fit method leveraged Band 7 of the Landsat ETM+ data, which was particularly sensitive to hydroxyl alterations. This band, when combined with Band 3 (representing iron oxide minerals) and Band 4 (representing vegetation cover), provided valuable information for identifying zones enriched in clay minerals. While LS-Fit is often associated with higher spectral resolution data, such as ASTER, it can still be effectively applied to Landsat ETM+ data for minerals with distinct spectral features within the available bands. In this case, Band 7's sensitivity to hydroxyl absorption made it suitable for detecting clay minerals.

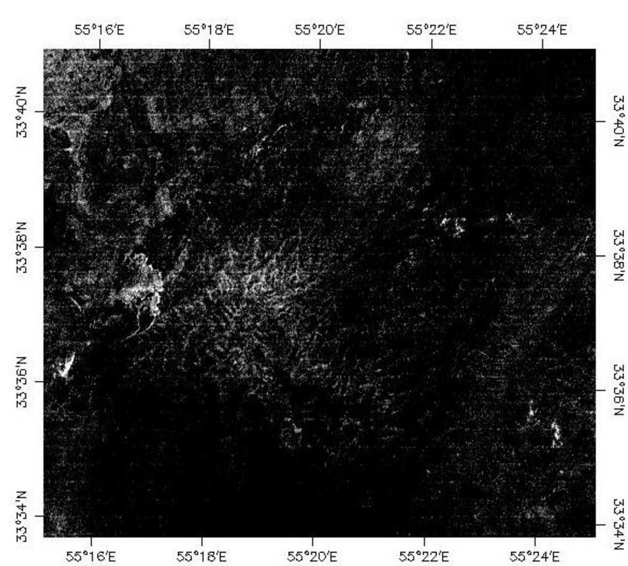

Fig. 6. The PC3 image highlighting iron oxide minerals, with altered regions shown as bright pixels.

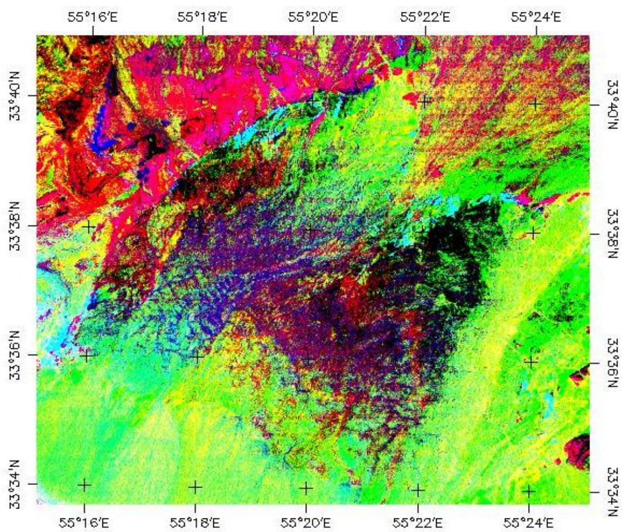

Fig. 7. The RGB (432) colour composite image obtained by the Crosta technique. OH-type alterations are displayed in red to orange colour.

Fig. 8 visually shows these promising zones identified through the LS-Fit method using the Band 7 as model band. The image clearly highlights areas with potential for clay mineral alteration as bright pixels, providing valuable information for further field investigations.

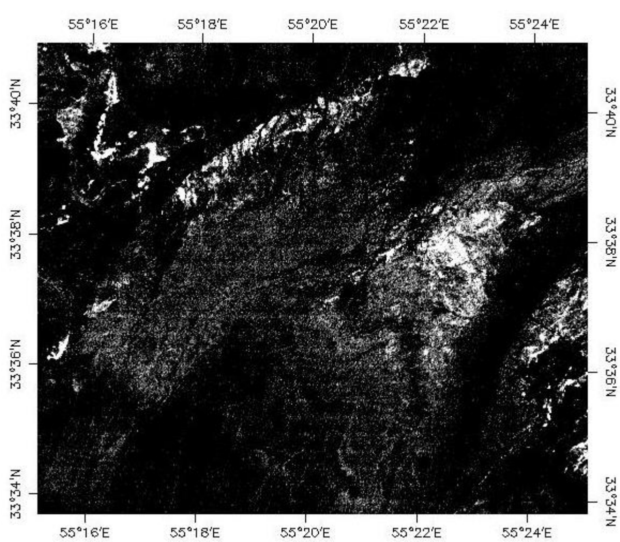

Fig. 8. Image obtained by the LS-Fit technique for clay minerals as bright pixels.

5.3.2. Iron oxide mineral alterations

In addition to clay minerals, iron oxide minerals play a crucial role as indicators of hydrothermal alteration zones. The examples of these minerals include iron oxides like hematite and goethite, and sulfates, such as jarosite, which commonly form from the weathering of sulfides in epithermal environments.

To identify areas with iron oxide alterations, the LS-Fit method focused on Band 3 of the Landsat ETM+ data as the model band. This band exhibits high reflectance from iron oxides, making it a valuable tool for their detection. Since no negative operation was needed for this band, the target points related to iron oxide alterations appeared as luminous pixels in the processed image.

Fig. 9 presents a grayscale representation of the residual component from the LS-Fit analysis on Band 3, highlighting these areas of potential iron oxide alteration. By analyzing the distribution and intensity of these bright pixels, we can further refine our understanding of the hydrothermal alteration processes within the study area.

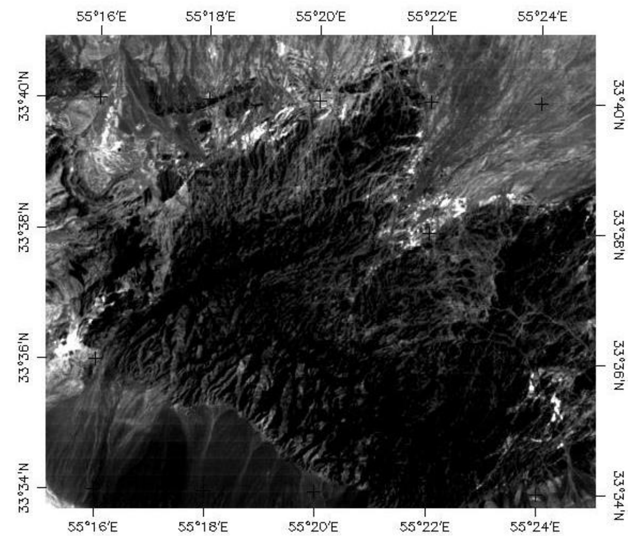

Fig. 9. Display of the residual component from LS-Fit analysis on band 3. Iron oxide alterations shown as bright pixels.

5.4. Providing promising points

The enhanced Crosta technique offers a significant advantage by allowing the simultaneous visualization of both iron oxide and clay alteration signatures within a single composite image. To achieve this, we performed a second PCA directly on the results obtained from the initial PCA analysis. As described earlier, this involved creating an RGB color composite image using specific principal components:

R: PC4 (OH) - representing hydroxyl-bearing minerals

G (Green): PC3 (OH) - further highlighting hydroxyl alterations

B (Blue): PC2 (Fe) - representing iron oxide minerals

The RGB composite image allowed for a more comprehensive interpretation of the alteration patterns. By analyzing the variations in color and intensity, we identified some promising points as bright blue pixels exhibiting strong alteration signatures. These points represent areas potentially associated with bentonite mineralization and warrant further investigation (Fig. 10).

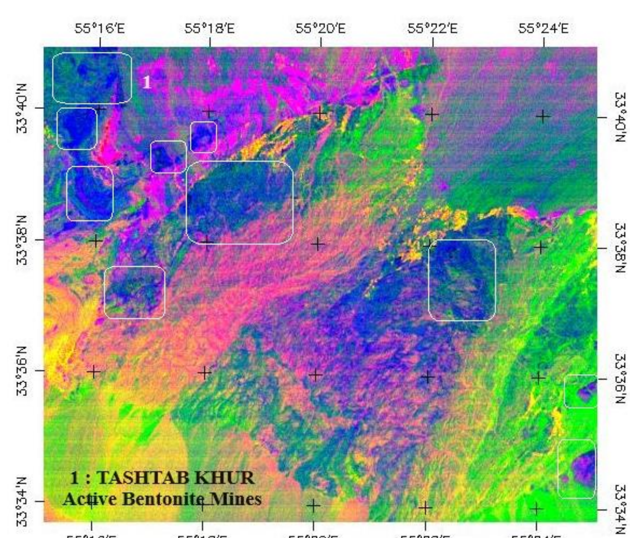

Fig. 10. The locations of promising points as blue pixels identified for potential bentonite mineralization using the enhanced Crosta technique.

6. Field investigation

To validate the remote sensing results, a field investigation was conducted at central points exhibiting strong alteration signatures. At these points, representative rock samples were collected from some of the areas showing visible alteration (Figs. 12 and 13). The common method for identifying clay minerals is using the XRD analysis. The paragenesis of minerals in the region includes smectite, quartz, kaolinite, calcite, dolomite, and opal cristobalite. The results confirmed the presence of smectite (montmorillonite), indicating significant bentonite (Fig. 14).

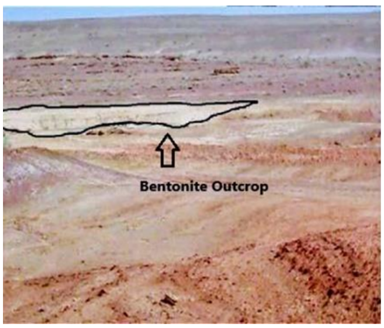

A

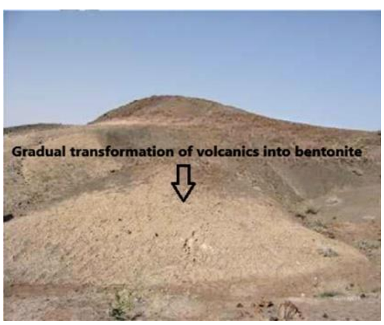

B

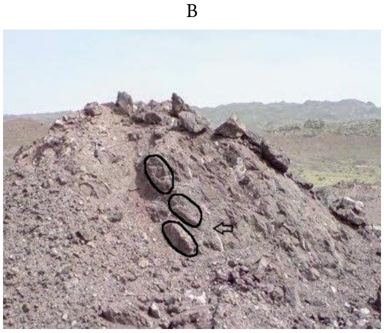

C

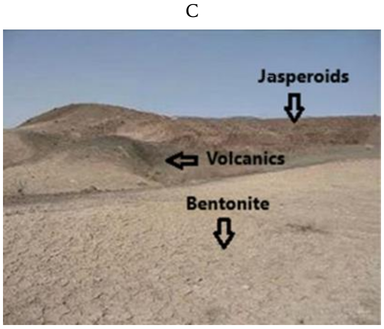

D

Fig. 12. .A) Bentonite outcrop in the region, B) The gradual transformation of volcanics into bentonite, C) The pillow form of the region's volcanics, and D) The general view of the region including volcanics next to bentonites and Jasperoid masses

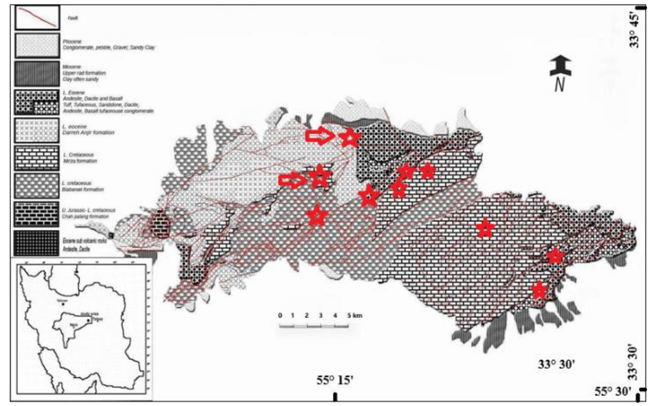

Fig. 13. The geological map of the area, UTM Zone 40 S. The promising points and sampling locations are marked on the map.

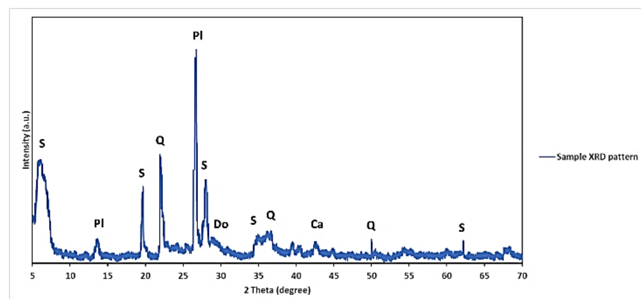

Fig. 14. The XRD of prepared sample where S=Smectite, Q=Quartz, Pl=Plagioclase, Ca=Calcite, and Do=Dolomite.

7. Conclusion

This study demonstrated that satellite imagery is highly effective in the initial phase of mineral exploration. It plays a crucial role in identifying hydrothermal alterations, delineating mineral deposits, and locating key mineralization indicators, including contact zones, linear, and circular patterns. The integrated approach of using the LS-Fit method and the enhanced Crosta technique, in conjunction with field validation, proved successful in identifying potential bentonite deposits. ETM+ data effectively identified minerals containing hydroxyl groups and iron oxides, leading to the identification of prospective exploration sites. Given the presence of active bentonite deposits in the region and the promising laboratory results, further field investigations and sampling are recommended. This approach offered clear advantages over previous studies in the region, particularly in terms of cost-effectiveness and efficiency in the initial stages of exploration.

Future research should prioritize expanding the study area and incorporating higher-resolution imagery, such as ASTER (with its higher spectral resolution), particularly in the SWIR region, Landsat 8/9, or Sentinel 2. The comparative analysis of alteration mapping accuracy using these different data sources, as demonstrated by Esmaelzadeh Kalkhoran et al. (2024) [24], should be conducted. In addition, more extensive field validation, including geochemical analysis using the XRD or Scanning Electron Microscopy (SEM), is needed to refine our understanding of the spatial distribution and economic viability of bentonite resources in this region and other areas with similar geological settings. Furthermore, future investigations should explore the integration of alternative methods, such as the Spectrum-Area fractal model combined with the TOPSIS decision-making method (previously used for delineating iron alteration zones [25]), and the integration of SFF and fractal modelling approaches, similar to the methods applied by Behbahani et al. [26], with the techniques presented in this study to further enhance mineral exploration accuracy.

Acknowledgements

This research did not receive any specific grant from funding agencies in the public, commercial, or not-for-profit sectors.

Data availability statement

The data that support the findings of this study are available from the corresponding author upon reasonable request.

References

[1]. Oppenheimer C. SABINS, FF 1997. Remote Sensing. Principles and Interpretation, xiii+ 494 pp. New York: WH Freeman & Co. Price£ 32.95 (hard covers). ISBN 0 7167 2442 1. Geological Magazine. 1998;135(1):143-58.

[2]. MalekMahmoudi F. Mineralogical and geochemical studies of hydrothermal alteration and mineralization of altered zones in Tashtab Mount, Khur (North East of Isfahan): Isfahan University; 2010.

[3]. Marjoribanks R. Geological methods in mineral exploration and mining: Springer Science & Business Media; 2010.

[4]. Lamrani O, Aabi A, Boushaba A, Seghir MT, Adiri Z, Samaoui S. Bentonite clay minerals mapping using ASTER and field mineralogical data: a case study from the eastern Rif belt, Morocco. Remote Sensing Applications: Society and Environment. 2021;24: 100640.

[5]. Van der Meer FD, Van der Werff HM, Van Ruitenbeek FJ, Hecker CA, Bakker WH, Noomen MF, et al. Multi-and hyperspectral geologic remote sensing: A review. International journal of applied Earth observation and geoinformation. 2012;14(1):112-28.

[6]. Saed S, Azizi H, Daneshvar N, Afzal P, Whattam SA, Mohammad YO. Hydrothermal alteration mapping using ASTER data, Takab-Baneh area, NW Iran: A key for further exploration of polymetal deposits. Geocarto International. 2022;37(26):11456-82.

[7]. Mirsepahvand F, Jafari M, Afzal P, Arian MA. Identification of Alteration Zones using ASTER Data for Metallic Mineralization in Ahar region, NW Iran. Journal of Mining and Environment. 2022;13(1):309-24.

[8]. Gholami R, Moradzadeh A, Yousefi M. Assessing the performance of independent component analysis in remote sensing data processing. Journal of the Indian Society of Remote Sensing. 2012;40: 577-88.

[9]. Ciampalini A, Garfagnoli F, Del Ventisette C, Moretti S. Potential use of remote sensing techniques for exploration of iron deposits in Western Sahara and Southwest of Algeria. Natural resources research. 2013;22: 179-90.

[10]. Gupta RP. Remote sensing geology: Springer; 2017.

[11]. Alimohammadi M, Alirezaei S, Kontak DJ. Application of ASTER data for exploration of porphyry copper deposits: A case study of Daraloo–Sarmeshk area, southern part of the Kerman copper belt, Iran. Ore geology reviews. 2015;70: 290-304.

[12]. Amer R, El Mezayen A, Hasanein M. ASTER spectral analysis for alteration minerals associated with gold mineralization. Ore Geology Reviews. 2016;75: 239-51.

[13]. Singh A, Harrison A. Standardized principal components. International journal of remote sensing. 1985;6(6):883-96.

[14]. Crosta A, De Souza Filho C, Azevedo F, Brodie C. Targeting key alteration minerals in epithermal deposits in Patagonia, Argentina, using ASTER imagery and principal component analysis. International journal of Remote sensing. 2003;24(21):4233-40.

[15]. Crosta AP, editor Enhancement of Landsat Thematic Mapper imagery for residual soil mapping in SW Minas Gerais State Brazil, a prospecting case history in greenstone belt terrain. Proceedings of the 7th ERIM Thematic Conference on Remote Sensing for Exploration Geology, 1989; 1989.

[16]. Loughlin W. Principal component analysis for alteration mapping. Photogrammetric Engineering and Remote Sensing. 1991;57(9):1163-9.

[17]. ESMAELZADEH KALKHORAN S, Ghannadpour SS, Jalili H, Moeini Rad A. Investigating porphyry copper alterations and spectral behavior of related minerals using ASTER satellite images in the Zafarghand region, Isfahan. Advanced Applied Geology. 2024;14(3):623-51.

[18]. Ghannadpour SS, Hasiri M, Jalili H, Talebiesfandarani S. Satellite Image Processing: Application for Alteration Separation based on U-Statistic Method in Zafarghand Porphyry System (Iran). Journal of Mining and Environment. 2024;15(2):667-81.

[19]. Ghannadpour SS, Esmailzadeh Kalkhoran S, Jalili H, Behifar M. Delineation of mineral potential zone using U-statistic method in processing satellite remote sensing images. International Journal of Mining and Geo-Engineering. 2023;57(4):445-53.

[20]. Ghannadpour SS, Hasiri M, Shahrabi HS, Jalili H. Mapping alteration zones associated with Cu mineralization: An approach based on image processing using the singularity method and fuzzy gamma operator. Kharazmi Journal of Earth Sciences. 2024;10(1):91-122.

[21]. Ghannadpour SS, Hasiri M, Jalili H, Salehi Shahrabi H. Identifying alterations of Zafarghand porphyry copper system (Isfahan): employing singularity method and false color composite. International Journal of Mining and Geo-Engineering. 2024;58(3):315-22.

[22]. Rothery D. Improved discrimination of rock units using Landsat Thematic Mapper imagery of the Oman ophiolite. Journal of the Geological Society. 1987;144(4):587-97.

[23]. Ghannadpour SS, Esmaelzadeh Kalkhoran S, Behifar M, Jalili H. Delineation of the alteration zones by CN fractal model on ASTER images. Journal of Mining and Environment. 2024.

[24]. Esmaelzadeh Kalkhoran S, Ghannadpour SS, Moeini Rad A, Jalili H. Comparing the performance of ASTER and LANDSAT 8 satellite images in identifying iron oxide and porphyry copper alterations in Zafarghand region of Isfahan province. Journal of Mineral Resources Engineering. 2024;9(1):41-65.

[25]. Pourgholam MM, Afzal P, Adib A, Rahbar K, Gholinejad M. Delineation of Iron alteration zones using spectrum-area fractal model and TOPSIS decision-making method in Tarom Metallogenic Zone, NW Iran. Journal of Mining and Environment. 2022;13(2):503-25.

[26]. Behbahanı B, Haratı H, Afzal P, Lotfı M. Determination of alteration zones applying fractal modeling and Spectral Feature Fitting (SFF) method in Saryazd porphyry copper system, central Iran. Bulletin of the Mineral Research and Exploration. 2023;172(172):1-14. [